geoconvention
Calgary • Canada • May 15-17 2023

Towards improving crosstalk suppression in multiparameter FWI by decorrelating parameter classes

Mariana Lume, Scott Keating, and Kris Innanen
CREWES, University of Calgary

Summary

Multiparameter FWI is commonly affected by parameter crosstalk. These effects are described by the Hessian, which also impacts the shape of the objective function iso-surfaces and the convergence of the optimization algorithms. This study focuses on finding an intermediate model space where the parameter classes are decorrelated, i.e., where the Hessian is an identity matrix, to minimize crosstalk and reach an accurate minimum that could be transformed to the ρ, V_P, and V_S model space. Transformation rules between model spaces were applied using transformation matrices (**T**) constructed to satisfy constraints imposed by the Hessian of the intermediate system. Overall, this FWI method produced good V_S estimations but did not overcome a reference FWI in the V_P and ρ results, since more crosstalk was introduced. However, improvements on the structure of the Hessians were brought for some areas of the mesh, which makes the decorrelation ideas promising to minimize these coupled effects. The drawbacks were related to a localized approach used to compute **T**, which, in future work, might need to consider the crosstalk contributions of multiple grid cells.

Introduction

Crosstalk between parameters of different classes means that different physical properties are confused in the inversion, yielding poorly accurate results and convergence slowness (Operto et al., 2013; Keating and Innanen, 2019). A common strategy to mitigate these effects is to design FWI workflows based on minor correlation of radiation patterns of a set of parameters. Additionally, these coupled effects are quantified by the Hessian, whose structure impacts the objective function iso-surfaces and therefore the convergence of the optimization algorithms (Innanen, 2020c). Thus, crosstalk suppression could be achieved with the manipulation of the Hessian, since no parameter correlation would exist if it had an identity matrix structure or a multiple of it (Operto et al., 2013; Métivier et al., 2015). Therefore, the objective of this study was to obtain crosstalk corrected values of V_p, V_s, and density (ρ) by performing a frequency domain FWI for an intermediate set of parameters that ideally should not contain any leakage, since its Hessians are expected to approximate the identity matrix.

Background

In the isotropic elastic scenario, the medium is characterized by the density ρ and the Lamé parameters λ and μ. Here, the wave equation described by Pratt (1990) can be written in matrix form as:

$$\rho\omega^2\boldsymbol{u} + c_{11}\nabla(\nabla\cdot\boldsymbol{u}) - c_{44}\nabla\times(\nabla\times\boldsymbol{u}) + \nabla(c_{11} - 2c_{44})(\nabla\cdot\boldsymbol{u}) + \nabla c_{44}(\nabla\boldsymbol{u} + \nabla\boldsymbol{u}^T) + \boldsymbol{f} = 0 \quad (1)$$

where ω is the angular frequency, **u** is the particle displacement vector, **f** is the source term and $c_{11} = \lambda + 2\mu$ and $c_{44} = \mu$. Although c_{11}, c_{44}, and ρ is the root parameterization, Equation 1 can adopt any other 3 elastic parameters that are related to them. In the case of the ρ, V_P, and V_S, these relationships are:

$$c_{11} = {V_P}^2\rho; \quad (2) \qquad c_{44} = {V_S}^2\rho \quad (3)$$

Moreover, each re-parameterization is a transformation between coordinate systems (Innanen, 2020a, b, c, d). To change to a different model space, we must consider that the objective function (φ) is a scalar quantity and is invariant under transformations. However, the model updates are vectors that change under transformations. Hence, to map a contravariant vector from an initial system *s* to a new system *r* and backwards, these rules are necessary:

$$s^\nu = t^\nu_\mu r^\mu; \quad (4) \qquad r^\nu = (t^{-1})^\nu_\mu s^\mu \quad (5)$$

where **T** (*t* in indicial notation) is a transformation matrix constructed to produce iso-surfaces of φ with a particular shape in the transformed model space. Since scalar quantities do not change under transformations, finding the minimizer of φ in the *r* space is equivalent to finding it in the *s* system.

On the other hand, the linear form of the Gauss-Newton approximation of the Hessian is:

$$H_{(i,j),(k,l)} = \left(\frac{\boldsymbol{\partial d_p}}{\boldsymbol{\partial s_{i,j}}}\right)\left(\frac{\boldsymbol{\partial d_p}}{\boldsymbol{\partial s_{k,l}}}\right)^* \qquad (6)$$

Where d_p corresponds to the predicted data and *j, l* refer to the parameter class and *i*, *k* to the position. Figure 1 shows the full Hessian organized in 3x3 blocks; when the parameter classes are not the same (*j* ≠ *l*), i.e., off-diagonal blocks, the full Hessian describes the existing trade-off. Then, no coupled effects between parameters of different classes would exist if these values were zero. If the values of the full Hessian are extracted at a fixed position per block, a local 3x3 matrix can be formed (Point-wise Hessian), characterizing the crosstalk between parameters of different classes only at that location. Moreover, the same figure illustrates that if we perturb the parameter classes at one fixed position and want to study the change of the gradient in all locations for all parameter classes, vertical profiles across the selected location can be extracted and, by reshaping them per block of the full Hessian, a point-probes Hessian can be constructed.

Similarly, when φ has ellipsoidal iso-surfaces with eccentricities and misalignments, the parameter information is mixed due to problems encountered by the Steepest Descent method to reach the global minimum. Innanen (2020a and c) proved that, for a quadratic objective function, the Steepest Descent and the Gauss-Newton updates are parallel, if the Hessian behaves as an identity matrix, reaching a more accurate local minimum. Hence, we can design transformation matrices that meet those constraints by solving the transformation rules for the Hessian (Innanen, 2020c):

$$t^\lambda_\mu H_{\lambda\sigma}(s) t^\sigma_\nu = H_{\mu\nu}(r) = \delta_{\mu\nu} \quad (7)$$

Workflow

The applied FWI workflow is observed in Figure 2. The optimization algorithm used was Steepest Descent and a multiscale approach was executed with 8 groups of 4 frequencies each, with values from 1 to 20Hz. The main assumption was to work with a point-wise Hessian of the *s* model space to find the **T** matrix that transforms it into an identity matrix in the *r* model space, as a first attempt to make the process computationally feasible. Additionally, Hessians computed with the final estimates were analyzed to determine how close they were to the sought identity matrix. To achieve this, we used an evaluation metric consisting of a 3x3 matrix formed after computing the norm of each block of a studied point-probes Hessian to capture the existent crosstalk between parameters of different classes in all the mesh and not only at the location selected to compute **T**. The closer to zero the off-diagonal terms of this matrix, the less crosstalk between parameters of different classes is encountered in all locations.

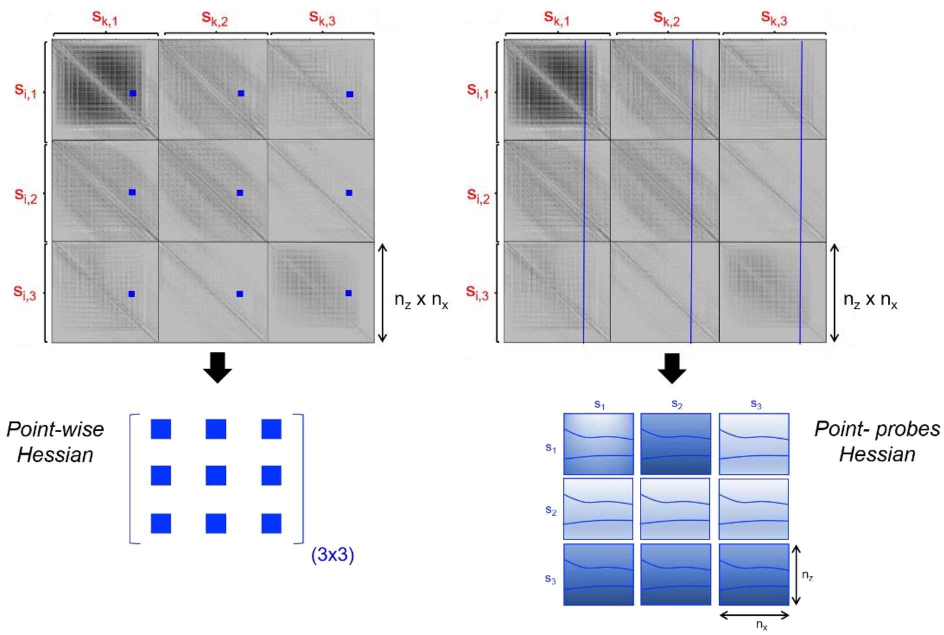

Figure 1. Illustration of a full Hessian, modified from (Métivier et al., 2015), and how a point-wise and a point-probes Hessian can be constructed from it; n_z and n_x are the number of samples in the vertical and horizontal direction of the model grid, respectively.

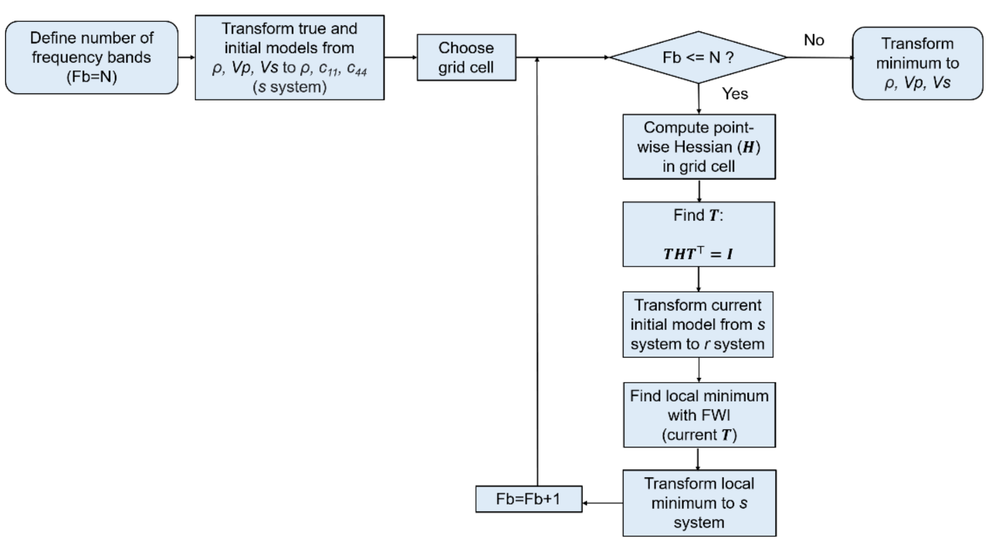

Figure 2. Re-parameterized FWI workflow followed in this study.

Results

A series of sources and receivers were placed at the top of the model grid, but also some receivers were placed at the bottom to enhance the illumination of the heterogeneities. Figure 3a shows the true values of ρ, V_P, and V_S. Two types of FWI were performed: (1) a reference inversion, i.e., without applying any transformation rule, and (2) an inversion with the proposed workflow; both with the same frequency bands, initial models, optimization strategy, and number of iterations. Figure 3b illustrates the results obtained without applying transformation rules. Noticeable crosstalk effects are observed around the ρ anomaly and subtle crosstalk is seen below the V_P heterogeneity. The models estimated with the re-parameterized FWI are shown in Figure 3c. This time, much more crosstalk was encountered around the ρ and V_P heterogeneities.

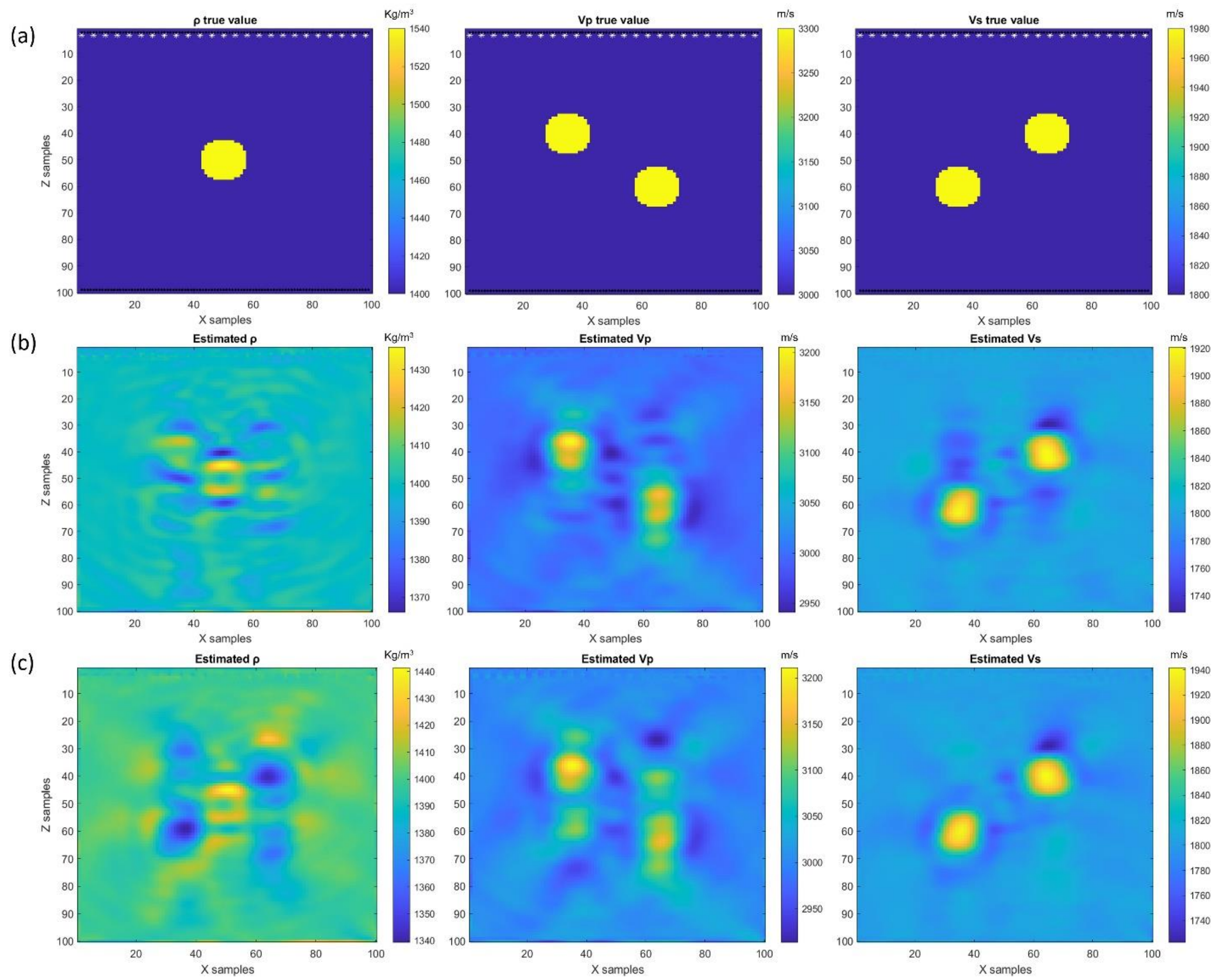

Figure 3. (a) True ρ, V_P, and V_S models. (b) Models estimated with a baseline FWI, i.e., without re-parameterization. (c) Models estimated with a re-parameterized FWI after selecting location x=50 and z=20 to compute **T**.

The point-probes and point-wise Hessian, as well as the normalized crosstalk metric computed with the estimates from the reference inversion are observed in Figure 4. Overall, the local

Hessian had a structure distant from the identity matrix. Moreover, the crosstalk metric showed a similar organization of the values, with strong crosstalk between ρ and V_P and between ρ and V_S, but much less between V_P and V_S, in all locations, as is expected for this model space.

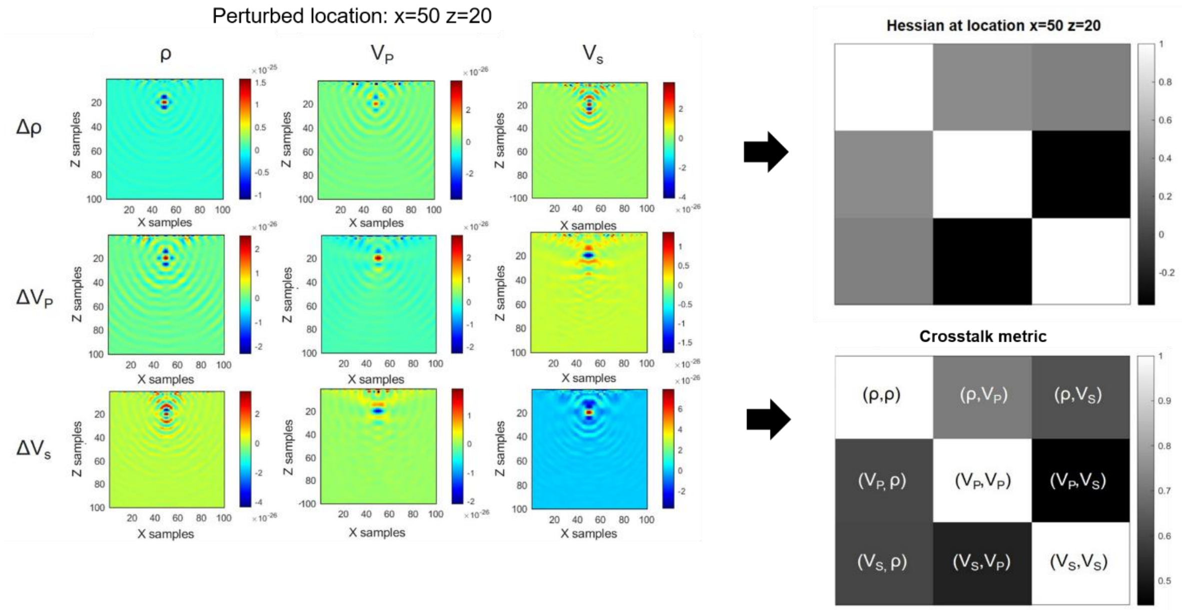

Figure 4. Point-probes Hessian computed with baseline estimates. The 3x3 matrix on top is the local Hessian at the perturbed grid cell. The 3x3 matrix at the bottom is the crosstalk metric calculated from the shown point-probes Hessian.

The Hessians and crosstalk metric computed in the *r* model space with the estimates from the re-parameterized inversion are observed in Figure 5. The identity matrix structure was observed only at and close to the grid cell chosen to compute **T**, not in the entire mesh. Outside this small area, different correlation patterns appeared in the blocks of the point-probes Hessian. Hence, this explains why the crosstalk metric summarized a noticeable trade-off between model parameters in all the grid cells.

Conclusions

After treating the FWI re-parameterization as a coordinate transform problem and seeking parameters where the Hessian is the identity matrix by designing transformation matrices (**T**) based on single points, a new model space where the parameter classes were decorrelated was found, but only in locations close to the grid cell chosen to compute **T**, losing this structure as we get distant from the location and introducing coupled effects between parameters of different classes. The obtained results indicate that a different numerical procedure to compute **T** should be a matter of future investigation, aiming to produce a more constant identity structure in all locations by considering the contribution of crosstalk in multiple grid cells and not only at a fixed point, for instance by using the point-probes Hessian to design the transformation matrices.

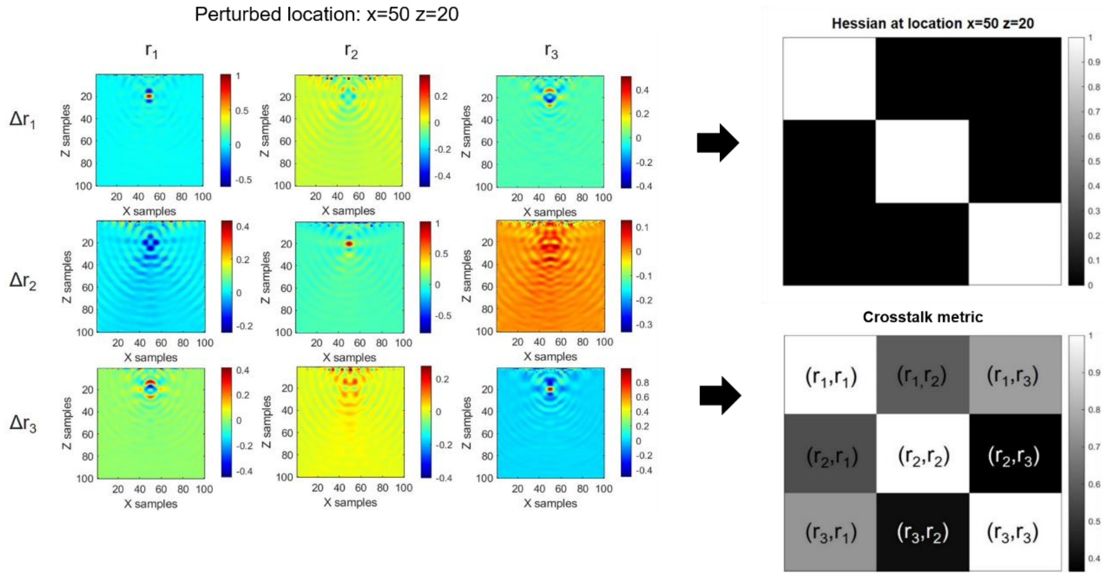

Figure 5. Point-probes Hessian computed with estimates obtained from a re-parameterized FWI. The 3x3 matrix on top is the local Hessian at the perturbed grid cell. The 3x3 matrix at the bottom is the crosstalk metric calculated from the shown point-probes Hessian.

Acknowledgments

The authors would like to thank the sponsors of the CREWES project as well as the NSERC (Natural Science and Engineering Research Council of Canada) under the grant CRDPJ 543578-19 for making this work possible through their financial support.

References

Innanen, K., 2020a, Application of misfit-based model space coordinate system design to seismic AVO inversion: CREWES Research Report, 32, No. 28.

Innanen, K., 2020b, Application of misfit-based model space coordinate system design to seismic full waveform inversion: CREWES Research Report, 32, No. 29.

Innanen, K., 2020c, Model re-parameterization via misfit-based coordinate transforms: CREWES Research Report, 32, No. 30.

Innanen, K., 2020d, A review of tensors in non-cartesian coordinate systems: CREWES Research Report, 32, No. 27.

Keating, S., and Innanen, K., 2019, Parameter cross-talk and leakage between spatially-separated unknowns in viscoelastic full waveform inversion: CREWES Research Report, 31, No. 35.

Métivier, L., Brossier, R., Operto, S., and Virieux, J., 2015, Acoustic multi-parameter FWI for the reconstruction of p-wave velocity, density and attenuation: preconditioned truncated newton approach: SEG Expanded Abstracts, 1198–1203.

Operto, S., Gholami, Y., Prieux, V., Ribodetti, A., Brossier, R., Métivier, L., and Virieux, J., 2013, A guided tour of multiparameter Full-Waveform Inversion with multicomponent data: From theory to practice: The Leading Edge, 1040–1054.

Pratt, R. G., 1990, Frequency-domain elastic wave modeling by finite differences; a tool for crosshole seismic imaging: Geophysics, 55.